



Computational Hemodynamic Modeling of Arterial Aneurysms: A Mini-Review

Sarah N. Lipp^{1†}, Elizabeth E. Niedert^{1†}, Hannah L. Cebull¹, Tyler C. Diorio¹, Jessica L. Ma¹, Sean M. Rothenberger¹, Kimberly A. Stevens Boster^{1,2} and Craig J. Goergen^{1*}

¹ Weldon School of Biomedical Engineering, Purdue University, West Lafayette, IN, United States, ² School of Mechanical Engineering, Purdue University, West Lafayette, IN, United States

OPEN ACCESS

Edited by:

James B. Hoying,
Cardiovascular Innovation Institute
(CII), United States

Reviewed by:

Jessica E. Wagenseil,
Washington University in St. Louis,
United States
Jingyan Han,
Boston University, United States

*Correspondence:

Craig J. Goergen
cgoergen@purdue.edu

[†]These authors have contributed
equally to this work

Specialty section:

This article was submitted to
Vascular Physiology,
a section of the journal
Frontiers in Physiology

Received: 03 February 2020

Accepted: 09 April 2020

Published: 12 May 2020

Citation:

Lipp SN, Niedert EE, Cebull HL,
Diorio TC, Ma JL, Rothenberger SM,
Stevens Boster KA and Goergen CJ
(2020) Computational Hemodynamic
Modeling of Arterial Aneurysms: A
Mini-Review. *Front. Physiol.* 11:454.
doi: 10.3389/fphys.2020.00454

Arterial aneurysms are pathological dilations of blood vessels, which can be of clinical concern due to thrombosis, dissection, or rupture. Aneurysms can form throughout the arterial system, including intracranial, thoracic, abdominal, visceral, peripheral, or coronary arteries. Currently, aneurysm diameter and expansion rates are the most commonly used metrics to assess rupture risk. Surgical or endovascular interventions are clinical treatment options, but are invasive and associated with risk for the patient. For aneurysms in locations where thrombosis is the primary concern, diameter is also used to determine the level of therapeutic anticoagulation, a treatment that increases the possibility of internal bleeding. Since simple diameter is often insufficient to reliably determine rupture and thrombosis risk, computational hemodynamic simulations are being developed to help assess when an intervention is warranted. Created from subject-specific data, computational models have the potential to be used to predict growth, dissection, rupture, and thrombus-formation risk based on hemodynamic parameters, including wall shear stress, oscillatory shear index, residence time, and anomalous blood flow patterns. Generally, endothelial damage and flow stagnation within aneurysms can lead to coagulation, inflammation, and the release of proteases, which alter extracellular matrix composition, increasing risk of rupture. In this review, we highlight recent work that investigates aneurysm geometry, model parameter assumptions, and other specific considerations that influence computational aneurysm simulations. By highlighting modeling validation and verification approaches, we hope to inspire future computational efforts aimed at improving our understanding of aneurysm pathology and treatment risk stratification.

Keywords: hemodynamic modeling, computational fluid dynamics, aneurysm, validation, fluid-structure interaction

1. INTRODUCTION

Arterial aneurysms are pathological focal dilations of arteries that can have life-threatening consequences. Aneurysms are commonly classified as saccular (asymmetric outpouchings) or fusiform (circumferential dilations). Other distinct vascular pathologies include pseudoaneurysms, which are partial thickness dilations of the blood vessel wall, and arterial dissections, which occur when medial layers separate and pressurized blood extravasates into a false lumen (Kumar et al., 2018). Aneurysm complications include rupture, hypovolemic shock (Dawson and Fitridge, 2013;

Wanhainen et al., 2019), tissue compression (Thompson et al., 2015), dissection initiation or progression (Czerny et al., 2019), or thromboembolism and ischemia (Dawson and Fitridge, 2013; McCrindle et al., 2017). Aneurysm pathophysiology can involve endothelial changes, damage resulting in an inflammatory cascade, release of proteases, extracellular matrix remodeling, and smooth muscle cell apoptosis, all of which can propagate aneurysm growth and rupture (Chalouhi et al., 2012; Hendel et al., 2015) requiring surgical repair, coiling, and flow diverting stents (**Table S1**). Because there is abnormal blood flow and endothelial cell damage in aneurysms, coagulability can be pharmacologically altered to lower thrombus risk (McCrindle et al., 2017).

Current guidelines for aneurysm intervention consider diameter, expansion rate, symptoms, and other risk factors as summarized in **Table S1**. Since risk factors for aneurysm rupture prediction are imperfect considering that some small, growing aneurysms still rupture, it is likely that some large or rapidly growing aneurysms do not require surgical treatment (UCAS Japan Investigators et al., 2012; Dawson and Fitridge, 2013; Kontopodis et al., 2016; Saeyeldin et al., 2019). Similarly, the risk assessment of thromboembolism from aneurysms based on diameter has relatively poor sensitivity and specificity (Grande Gutierrez et al., 2019). However, assessing aneurysm hemodynamics with computational models may help identify more accurate predictors of vessel rupture or thrombosis formation, improving risk stratification that can guide clinical decision-making. This mini-review highlights recent literature that describes computational modeling of aneurysms and pseudoaneurysms using patient-specific geometries, boundary conditions, and model validation and verification.

2. FROM IMAGES TO SIMULATIONS

2.1. Imaging

Medical imaging can be used to acquire patient-specific information for computational fluid dynamics (CFD) and fluid-structure interaction (FSI) simulations. Vessel geometry information is often obtained using digital subtraction angiography (DSA), computed tomographic angiography (CTA), or magnetic resonance angiography (MRA). Recent efforts have also utilized volumetric ultrasound or optical coherence tomography to acquire vessel geometry (Jia et al., 2012; Van Disseldorp et al., 2019), but their application to CFD remains limited to animal studies (Phillips et al., 2017).

Every imaging technique has trade-offs. Most notably, DSA and CTA subject the patient to ionizing radiation, which can

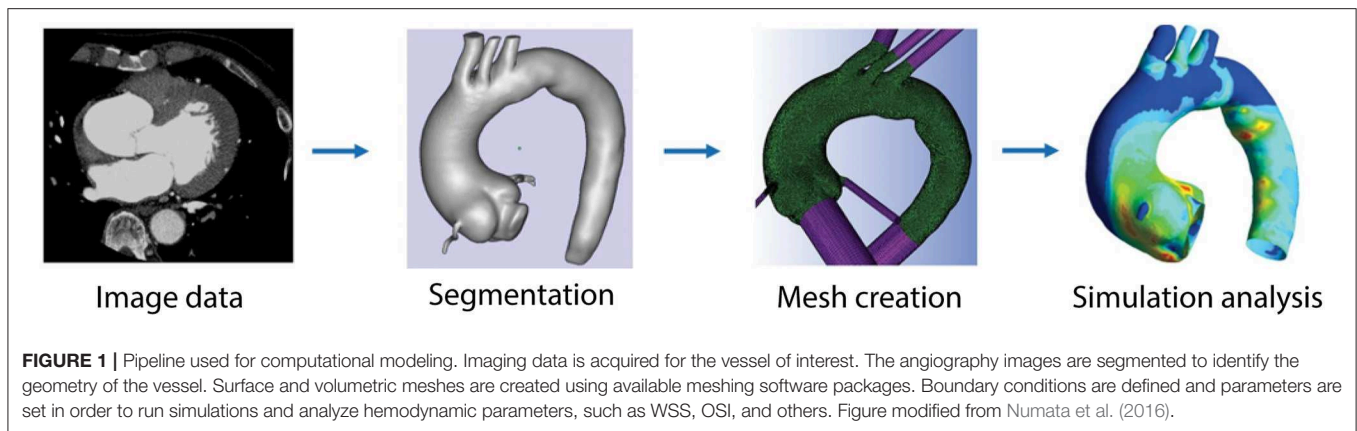
increase cancer incidence, limiting use for longitudinal studies (Einstein et al., 2007). Even so, the high resolution, low cost, and fast scan time have made CTA a common clinical imaging modality for aneurysms. While MRA does not subject patients to radiation, this technique requires expensive equipment, consists of longer scan times, and produces relatively low resolution images compared to CTA (Sailer et al., 2014).

In addition to aneurysm geometry, some imaging techniques provide subject-specific boundary conditions for hemodynamic simulations. Velocity information acquired non-invasively via pulsed wave Doppler ultrasound and phase contrast-magnetic resonance imaging (PC-MRI) can estimate two-dimensional velocity-based inlet boundary conditions (Boussel et al., 2009; Enevoldsen et al., 2012). PC-MRI provides time-resolved velocity measurements in either a single direction (2D PC-MRI) or throughout an entire volume (4D flow MRI) (Boussel et al., 2009; Eker et al., 2015), but is limited by lower spatio-temporal resolution. While each imaging modality has limitations, imaging data is key to provide the subject-specific information regarding aneurysm geometry and boundary conditions necessary for hemodynamic modeling.

2.2. Modeling

Three-dimensional computational simulations of the vasculature can be used to estimate hemodynamic metrics. If the walls of the model are rigid, only the fluid domain is considered. If the walls are compliant, both solid and fluid domains are considered, often referred to as FSI simulations. The fluid domain model can be created by segmenting the vessel lumen from medical imaging data (**Figure 1**). The entire volume is then typically broken into discrete elements, creating a mesh of individual nodes (**Figure 1**, third panel). The conservation of mass and momentum equations for pressure and velocity can then be solved at each spatial location within the domain (**Figure 2**). This process varies depending on the study, software, and methods used. The most common parameters, inputs, as well as how they are obtained are listed in **Table S2**. Hemodynamic parameters that may influence aneurysm formation, growth, rupture, and thrombosis can be calculated based on the simulation results (**Table S3**). For example, wall shear stress (WSS) is the tangential stress blood exerts on vessel walls and has been linked to rupture risk (**Figure 2B**; **Table S3**; Meng et al., 2014). For risk stratification studies, WSS-related parameters have been investigated (Liang et al., 2019), such as WSS gradient (WSSG) (**Table S3**; Longo et al., 2017) and oscillatory shear index (OSI). OSI represents the change in direction of the shear forces during the cardiac cycle, and elevated OSI is associated with pro-inflammatory markers (**Figure 2C**; Sei et al., 2017). Complex flow patterns are frequently observed in aneurysms (Xiang et al., 2011). Flow stagnation in an aneurysm can be quantified by the residence time (RT), which is the average time a particle remains within the aneurysm (Reza and Arzani, 2019). Higher RT indicates flow stagnation and retention of platelets and inflammatory cells, which may contribute to thrombus formation (**Figure 2D**; Rayz et al., 2010; Reza and Arzani, 2019).

Abbreviations: AAAs, abdominal aortic aneurysms; BAV, bicuspid aortic valve; CAAs, coronary artery aneurysms; CFD, computational fluid dynamics; CTA, computed tomographic angiography; DSA, digital subtraction angiography; FSI, fluid-structure interactions; IAs, intracranial aneurysms; KD, Kawasaki disease; MI, myocardial infarct; MRA, magnetic resonance angiography; MRI, magnetic resonance imaging; OSI, oscillatory shear index; PAAs, peripheral artery aneurysms; PDA, pancreaticoduodenal artery; PDAA, pancreaticoduodenal artery aneurysm; PC-MRI, phase contrast-magnetic resonance imaging; SMA, superior mesenteric artery; RT, residence time; TAAs, thoracic aortic aneurysms; WSS, wall shear stress; WSSG, wall shear stress gradient; VAAs, visceral artery aneurysms; VVUQ, verification, validation, and uncertainty quantification.



It is important to note that all models require assumptions, which can influence simulation results and model fidelity. This is especially important when estimating vessel wall properties, the inflow boundary conditions, and the outflow boundary conditions (Steinman and Pereira, 2019). While simulations are useful for calculating hemodynamic parameters linked to aneurysm progression, assumptions should be carefully considered to maintain reasonable model fidelity.

3. ANEURYSMS

3.1. Intracranial Aneurysm

Intracranial aneurysms (IAs) are present in 3.2% of the general population (Thompson et al., 2015). IAs are generally asymptomatic, but IA rupture can lead to subarachnoid hemorrhage (Thompson et al., 2015). While the management and risk stratification of IAs remains controversial (Cebal et al., 2011b) and there are no consensus guidelines with a diameter cut off (Thompson et al., 2015), a clinical standard for surgical intervention is defined as an aneurysm diameter ≥ 7 –10 mm (Bederson et al., 2000; Thompson et al., 2015).

Patient-specific CFD simulations are now being used to identify hemodynamic parameters that may trigger IA growth or rupture (Etminan and Macdonald, 2015) (Figures 2A–D). Studies considering thrombosis often report RT, recirculation zones, and/or WSS as these are of interest for growth and rupture analyses (Vali et al., 2017). Initial conflicting results were reported for IA suggesting that aneurysm progression is related to both low WSS (Boussel et al., 2008; Miura et al., 2013) and high WSS (Cebal et al., 2009, 2011b). A unified theory by Meng et al. (2014) proposes two independent progression pathways. The first suggests that high WSS and a positive WSSG make a region prone to dilation, while the other suggests low WSS and high OSI are the driving forces. More recent work has correlated aneurysm growth and rupture to high OSI (Kawaguchi et al., 2012), high WSSG (Shojima et al., 2010; Machi et al., 2017), and larger areas of low WSS (Zhang et al., 2016; Qiu et al., 2017). Given that abnormally low WSS is related to endothelial cell damage, areas of low WSS may also correlate to areas of further vascular wall damage. Cebal et al. (2011b) identified additional qualitative risk factors within the aneurysmal region, including complex

flow, unstable flow structures, concentrated inflows, and small impingement regions. Recent advancements in IA modeling have yielded the ability to aid in surgical planning and improve patient outcomes in several case studies (Vali et al., 2017). The ultimate aim to predict IA rupture risk on a patient-specific basis remains a work in progress (Saqr et al., 2019).

Unique challenges exist for modeling IAs. The small size of the cerebral vasculature makes accurate vessel segmentation and velocity measurements difficult. Although the cerebral vasculature is less elastic than proximal elastic arteries, a rigid wall assumption can alter WSS values and increase flow instability (Torii et al., 2007; Yamaguchi, 2016). Finally, a Newtonian blood flow assumption may be insufficient in some IA cases (Saqr et al., 2019). Similar to aneurysms in other parts of the body, relevant assumptions and approximate error bounds should be reported to improve reproducibility when modeling IAs.

3.2. Thoracic Aortic Aneurysms

Thoracic aortic aneurysms (TAAs) are pathological dilations of the thoracic aorta, most commonly occurring in the ascending region (Isselbacher, 2005; Ramanath et al., 2009). Hypertension, aging, and smoking all contribute to risk of aortic aneurysm development, and single gene mutations have greater influence on TAA development than any other region of the aorta (Milewicz et al., 2008; Hiratzka et al., 2009; Pinard et al., 2019). Current clinical guidelines suggest that rupture risk outweighs surgical risk for non-familial cases when TAA diameter is ≥ 55 mm or expands at a rate ≥ 5 mm/year (Hiratzka et al., 2009; Erbel et al., 2014). However, dissection and rupture occasionally occur below these thresholds, demonstrating a critical need for improved risk assessment (Pape et al., 2007; Zafar et al., 2018).

Since the ascending thoracic aorta sits directly above the left ventricle, it typically experiences the highest blood velocities, wall forces, and wall displacements of any artery. Computational modeling can be used to simulate these forces either using a rigid wall assumption or FSI methods to incorporate the effects of wall elasticity—a critical aspect in highly deformable vessels like the aorta (Reymond et al., 2013; Trachet et al., 2015) (Figures 2E–H). Studies using a rigid wall often focus on geometric effects using patient-specific parameters without the additional computational

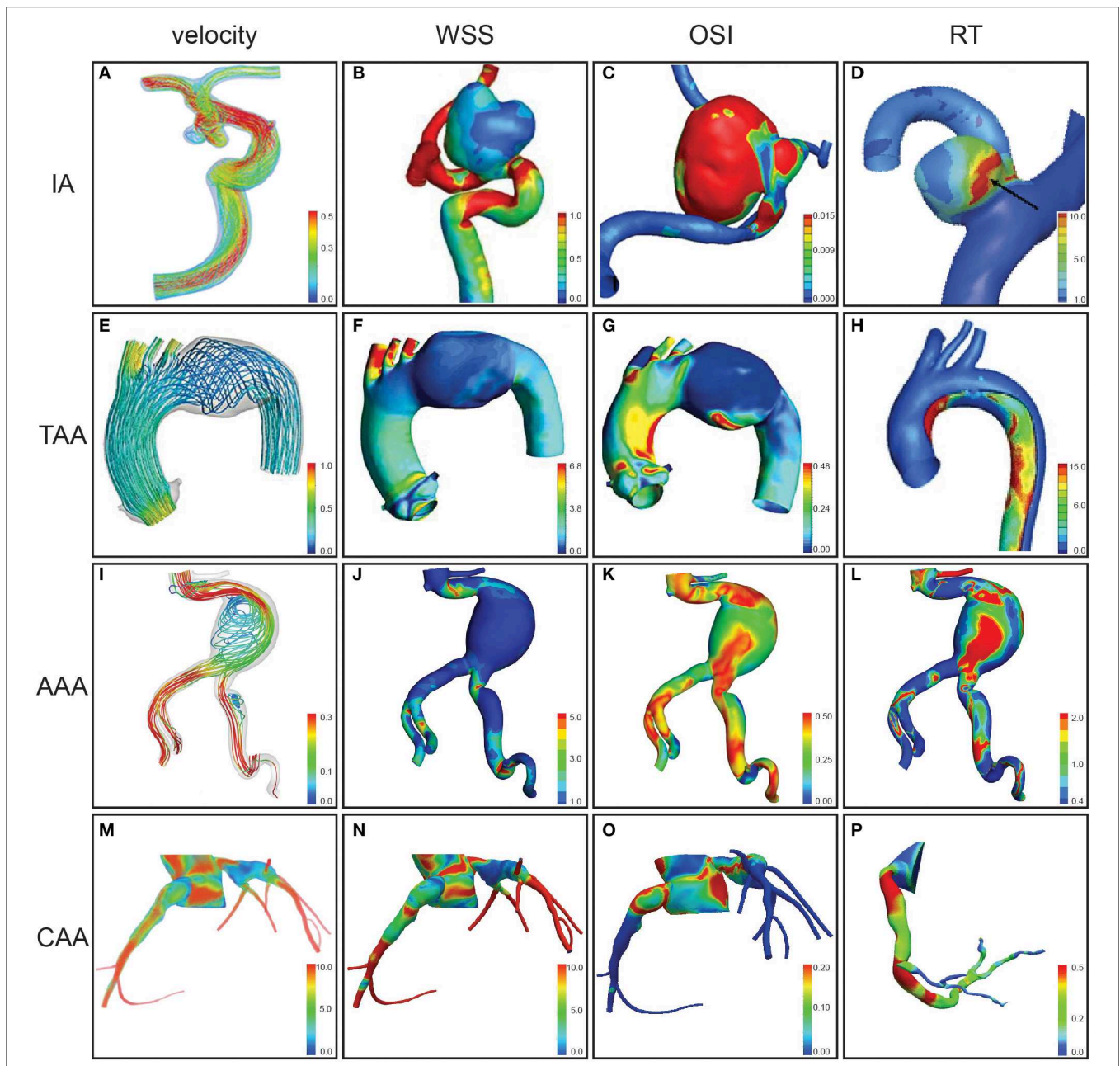


FIGURE 2 | Hemodynamic parameters assessed by computational modeling for aneurysms at different anatomical locations. Velocity (m/s) (**A**), velocity during peak systole (m/s) (**E,I**), velocity during diastole (cm/s) (**M**), wall shear stress (WSS) magnitude (**B**), WSS in peak systole (Pa) (**F**), WSS (Pa) (**J**), WSS in diastole (dynes/sq cm) (**N**), oscillatory shear index (OSI) (**C,G,K,O**), relative residence time (RT) (**D,H,L**), and particle RT gradient (s/m) (**P**) were assessed for intracranial aneurysms (IAs) of the internal carotid artery (**A**), paraclinoid aneurysm in a segment of internal carotid artery (**B,C**), and middle cerebral artery (**D**), distal arch thoracic aortic aneurysm (TAA) (**E-G**), thoracic aortic aneurysm dissection (**H**), abdominal aortic aneurysm (AAA) (**I-L**), and coronary artery aneurysms (CAAs) (**M-P**). Figures modified from Tian et al. (2016) (**A**), Wan et al. (2019) (**B-C**), Sugiyama et al. (2013) (**D**), Numata et al. (2016) (**E-G**), Shi et al. (2016) (**H**), Qiu et al. (2018) (**I-L**), Sengupta et al. (2012), Sengupta (2013) (**M-O**), and Sengupta et al. (2014) (**P**).

expense and required material properties needed for FSI. For example, studies using rigid walls revealed that patients with bicuspid aortic valve (BAV) have complex blood flow patterns that cause higher and uneven wall shear stresses, increasing the potential for TAA formation (Youssefi et al., 2017; Conde

mi et al., 2018; Edlin et al., 2019). Mendez et al. (2018) simulated blood flow in BAV TAAs using both rigid walls and FSI, finding non-significant differences in helical flow, but significantly lower estimated pressure in CFD simulations. In particular, they found the largest differences between rigid and deformable wall

simulations occur during peak systole when wall deformation is greatest. Another study focusing on effects of hypertension and wall stiffness found that stiffer TAAs were correlated with the largest amount of altered wall stress distributions (Campobasso et al., 2018). Taken together, these computational studies demonstrate the importance of subject-specific modeling when simulating TAA initiation, progression, wall stresses, and rupture risk.

3.3. Abdominal Aortic Aneurysms

The abdominal aorta is particularly susceptible to aneurysm development and rupture, causing 175,000 deaths around the world each year (McGloughlin and Doyle, 2010; Howard et al., 2015). Similar to TAAs, abdominal aortic aneurysms (AAAs) ≥ 50 – 55 mm in diameter or have an expansion rate ≥ 10 mm in a year are recommended for surgical intervention (Erbel et al., 2014; Chaikof et al., 2018; Wanhainen et al., 2019).

Recent works suggest that simulations can be used to better predict rupture risk when incorporating WSS compared to a diameter only metric, as the interaction between AAA hemodynamics and vascular biomechanics has a stronger influence on eventual rupture (Taylor and Steinman, 2010; Canchi et al., 2015) (Figures 2I–L). A study using an *in vitro* model showed that AAA WSS was negatively influenced by intimal thickness (Bonert et al., 2003); the inverse correlation between WSS and wall thickness increases the risk of the rupture. Inclusion of an intraluminal thrombus, which most AAAs contain, and major neighboring branching vessels additionally produced more accurate flow simulations (Vorp, 2007; Salman et al., 2019).

Another computational study investigated blood flow characteristics at the site of AAA rupture and found that more patients experienced rupture in regions with low WSS (Boyd et al., 2016). This could be due to the observation that zones of recirculation are correlated with abundant thrombus deposition (Boyd et al., 2016). Velocity streamline patterns, which represent particle trajectories, tend to be stronger near the middle of the aorta (Soudah et al., 2013). While different shear stress levels can activate different methods of platelet deposition, several studies found that sites of low WSS and vortex formation suggested thrombus formation (Biasetti et al., 2010, 2011). Soudah et al. (2013) discovered a correlation between degree of AAA asymmetry and asymmetric flow pattern within the sac, which may lead to higher risk of endothelial dysfunction, thrombus formation, and eventual rupture. Overall, these studies illustrate how computational modeling has furthered our understanding of AAA progression and rupture, and future AAA modeling studies will provide even more knowledge about this disease.

3.4. Peripheral and Visceral Aneurysms

Peripheral artery aneurysms are located in the axillary, brachial, carotid, subclavian, femoral, and popliteal arteries, while visceral artery aneurysms are located in the splenic, celiac, superior and inferior mesenteric, renal, and hepatic arteries (Anderson et al., 2013; Dawson and Fitridge, 2013). These aneurysms are relatively rare with visceral aneurysms affecting 0.01–0.2% of

the population (Huang et al., 2007). When detected, visceral aneurysms with a diameter ≥ 20 mm are typically treated to prevent rupture (Anderson et al., 2013). Peripheral aneurysms with a diameter ≥ 20 – 40 mm, depending on location, are treated to prevent thrombosis (Dawson and Fitridge, 2013). Idealized models of femoral artery pseudoaneurysms, where a saccular expansion develops often due to complications from percutaneous intervention, experience greater intraluminal pressures when the vessel to neck angle is larger (Suh et al., 2012). Further, simulations of common iliac artery aneurysms showed that as the size of the aneurysm increased, not only did WSS decrease, but remodeling of the upstream aorta also occurred (Parker et al., 2019). Finally, a study using pancreaticoduodenal artery aneurysm (PDAA) CFD models with superior mesenteric artery (SMA) occlusion resulted in analysis of the best treatment strategy. Surgery without revascularization could lead to recurrence of the PDAA, while revascularization could lead to high WSS and pressure (Li et al., 2019). These findings lead to stagnant flow in the pancreaticoduodenal artery (PDA), suggesting that revascularization can occlude the PDA and increase blood flow through the SMA (Li et al., 2019). Overall, the low prevalence, variation in anatomical location, and complex hemodynamics in peripheral and visceral vessels provide unique challenges when simulating blood flow. However, these lesions remain relatively under explored while still posing a clear risk to patients, highlighting the importance of studying hemodynamic changes via imaging and modeling to help improve clinical management.

3.5. Coronary Aneurysms

The incidence of coronary artery aneurysms (CAAs) is 1.65% (Abou Sherif et al., 2017). CAAs are found in patients with a history of Kawasaki disease (KD), a vasculitis, or atherosclerosis where the associated inflammatory processes weaken the vessel wall resulting in vessel dilation. CAAs can cause myocardial infarctions (MI) due to thrombosis (Abou Sherif et al., 2017). CAAs ≥ 8 mm in diameter or with a diameter z-score ≥ 10 are typically treated with anticoagulation therapy to prevent thrombus formation (McCrinkle et al., 2017). Computational modeling of CAAs has the potential to better risk stratify these lesions and influence medical management (Figures 2M–P).

The first KD patient-specific model of a CAA was reported in Sengupta et al. (2012). To investigate the role of aneurysm hemodynamic parameters and morphology, KD patient coronary arteries (Sengupta et al., 2014) and CAAs with virtually simulated increased aneurysm length (fusiform shape) (Grande Gutierrez et al., 2017) were modeled. Grande Gutierrez et al. (2017) found that increasing aneurysm length increased the area exposed to low WSS, suggesting fusiform CAAs may elevate thrombosis risk relative to saccular CAAs while also demonstrating a limitation of using diameter for risk stratification. Recently, models from 10 KD patients retrospectively showed WSS-derived parameters and RT had improved specificity without loss in sensitivity compared to diameter-based metrics for thrombotic risk stratification (Grande Gutierrez et al., 2019). Models from 61 patients with atherosclerosis-caused CAAs demonstrated that CAAs with a length/diameter ratio >2 have elevated WSS derived parameters

and increased incidence of MI (Fan et al., 2019). Together, these reports suggest that criteria based on diameter alone may be improved with additional simulation-based information.

While patient-specific computational modeling has the potential to better risk stratify coronary lesions, unique challenges exist when modeling CAAs. Specifically, the coronary arteries translate with cardiac motion and, unlike the rest of the systemic vasculature, diastolic blood flow is higher than systolic due to constriction of coronary vasculature when the heart contracts (Grande Gutierrez et al., 2019). Despite the use of diameter-based parameters for clinical risk stratification, fusiform aneurysms had non-significant increased risk of thrombosis compared to saccular CAAs (Sengupta et al., 2014). Future prospective studies with larger sample sizes could help determine the predictive clinical value of simulations when treating patients with these complex lesions.

4. VALIDATION

Subject-specific computational model utility is limited by the degree to which models accurately represent reality. Modeling protocol and assumptions can influence model fidelity, which is assessed through verification, validation, and uncertainty quantification (VVUQ). Verification addresses the degree to which a model accurately solves the governing equations, while validation addresses the appropriateness of the equations and boundary conditions employed in the model. Uncertainty quantification addresses how numerical and physiological variations influence model results. Standards for VVUQ are well-established in the computational fluid dynamics community (Roache, 1994, 1997; Babuska and Oden, 2004), and several recent reviews have addressed the topic in the context of cardiovascular modeling (Taylor and Steinman, 2010; Steinman and Migliavacca, 2018; Steinman and Pereira, 2019).

VVUQ of aneurysm CFD models has recently gained greater attention as the field has matured (Cebal et al., 2011a; Fiorella et al., 2011; Putman et al., 2011; Steinman, 2011). Campobasso et al. (2018) modeled ascending TAAs, both verifying and validating their results with 4D flow MRI. However, since imaging methods for directly validating CFD model results *in vivo* are fraught with uncertainty themselves, direct validation remains challenging (Augst et al., 2003; Bousset et al., 2009). One approach to validate computational models is to compare results with experimental measurements *in vitro*; however, this does not validate the impact of assumptions used to create the computational model, including segmentation-induced geometrical errors and assumptions regarding vessel wall properties and boundary conditions. Validation of patient-specific cardiovascular modeling remains a challenge since both *in vivo* and *in vitro* approaches to measuring velocity fields have inherent limitations.

“Challenges” are an alternative to direct validation where several groups analyze a common data set and compare results (Berg et al., 2015; Janiga et al., 2015; Voß et al., 2019). Challenges can indicate the extent and impact of modeling assumption variability, while also suggesting ways to normalize

to minimize variability in results. For example, Steinman et al. (2013) showed that differences in CFD solver settings on an IA model had relatively minor impact on peak systolic pressure drops (<8% variability) but significant impact on peak-systolic velocity entering the aneurysm sac. Valen-Sendstad et al. (2018) found large variability in sac-averaged WSS due to differences in segmentation, boundary conditions, and CFD solver settings that were reduced when normalizing by the parent vessel WSS. Voß et al. (2019) showed segmentation variability resulted in differences of 30% in mean aneurysmal velocity, 46% in neck inflow rate, and 51% in time-averaged WSS. Unlike most challenges, which do not have ground truth and therefore cannot assess accuracy, Berg et al. (2018) compared submitted geometries with higher resolution imaging data which served as the ground truth and validated that only one team correctly segmented the aneurysm necks. These reports suggest that multi-group, patient-specific modeling challenges can elucidate the impact of various modeling assumptions and suggest normalization approaches to better account for variability.

The degree to which computational models of arterial aneurysms have been validated varies widely with anatomical region; vascular territories where the field of computational modeling is more common and more mature tend to have more validation studies. For example, all of the modeling challenges mentioned were for IAs (Steinman et al., 2013; Berg et al., 2015, 2018, 2019; Janiga et al., 2015; Valen-Sendstad et al., 2018; Voß et al., 2019). Validation studies have also been performed for TAAs (e.g., Campobasso et al., 2018), AAAs (e.g., Kung et al., 2011), and CAAs (e.g., Kung et al., 2014), while the majority of modeling studies for PAAs and VAAs are case studies and generally do not include validation.

5. OUTLOOK

Although there is tremendous hope for the use of CFD modeling of aneurysms to aid in clinical decision making, there are only a few instances of CFD in surgical planning or large clinical cohort studies for aneurysms. The majority of studies have focused on predicting hemodynamics and not rupture risk stratification, especially for less common aneurysm locations, including PAA and VAA (Table S1). The conversion of hemodynamic values into clinically applicable parameters has been studied for IAs (Xiang et al., 2011; Detmer et al., 2018a,b), but most TAAs, AAAs, PAAs, VAAs, and CAAs studies are exploratory (Table S1). For CFD modeling of an aneurysm to be used widely in the clinic, large scale multi-centered studies and the identification of standardized parameters or groups of parameters that predict risk with high sensitivity and specificity are typically required (Kallmes, 2012). Additionally, the infrastructure to input patient-specific data and output a clinically relevant parameter also needs to be developed. As clinicians do not typically have time in their schedules to build CFD models and run simulations themselves (Singh et al., 2009), alternative approaches could involve the commercialization of a modeling service as done by HeartFlow[®] to identify patients with coronary artery disease that require treatment (Danad et al., 2017; Patel et al., 2020). Beyond

coronary disease, VASCOPS is a company that took a solid mechanics approach and developed A4clinics™ software using finite element modeling of the vessel wall to predict AAA rupture using Peak Wall Rupture Risk (VASCOPS, 2018). Its acceptance in the AAA field, however, has been limited as questions remain about clinical benefit (Chung et al., 2017; Boyd, 2020). For the widespread implementation of CFD modeling of aneurysms for clinical decision making, an artificial intelligence approach may be required followed by manual segmentation correction in order to handle a large number of cases (Taylor et al., 2018; Maher et al., 2019).

6. CONCLUSION

Computational modeling of the arterial systems is proving to be a valuable tool to study aneurysm growth, rupture, and thrombosis. Models can calculate hemodynamic parameters from complex geometries and have the potential to improve clinical decision-making. Common challenges include the incorporation of subject-specific boundary conditions, geometry, and error assessment due to modeling assumptions. Unique challenges exist in different anatomical locations, including vessel wall motion in TAAs and AAAs, flow during diastole in CAAs, anatomical variability in VAAs and PAAs, and anastomosis in IAs. The maturity of the field differs depending on location, from regions studied in depth, such as IAs and AAAs to more nascent areas, such as PAAs and VAAs (Table S1). Since predictive models are limited by the fidelity of the modeling assumptions, VUQ efforts provide critical assessment of the accuracy of

the model. As this field advances, more studies in diverse locations, use of large retrospective and prospective studies and longitudinal animal studies, and advancing from exploratory research to confirmatory studies could help fully capture the predictive value and clinical impact of computational hemodynamic modeling.

AUTHOR CONTRIBUTIONS

SL, EN, HC, TD, JM, SR, and KS wrote the sections of the manuscript. CG provided the initial guidance and edited all sections. All authors contributed to the manuscript revision and approved the submitted version.

FUNDING

Support for this review was provided by the Leslie A. Geddes Endowment at Purdue University.

ACKNOWLEDGMENTS

Initial input was provided by students in the Spring 2019 BME695 Cardiovascular Biomedical Engineering and Imaging class at Purdue University, in particular Tanmay Shidhore.

SUPPLEMENTARY MATERIAL

The Supplementary Material for this article can be found online at: <https://www.frontiersin.org/articles/10.3389/fphys.2020.00454/full#supplementary-material>

REFERENCES

- Abou Sherif, S., Ozden Tok, O., Taskoylu, O., Goktekin, O., and Kilic, I. D. (2017). Coronary artery aneurysms: a review of the epidemiology, pathophysiology, diagnosis, and treatment. *Front. Cardiovasc. Med.* 4:24. doi: 10.3389/fcvm.2017.00024
- Anderson, J. L., Halperin, J. L., Albert, N., Bozkurt, B., Brindis, R. G., Curtis, L. H., et al. (2013). Management of patients with peripheral artery disease (compilation of 2005 and 2011 ACCF/AHA guideline recommendations): a report of the American College of Cardiology Foundation/American Heart Association task force on practice guidelines. *J. Am. Coll. Cardiol.* 61, 1555–1570. doi: 10.1016/j.jacc.2013.01.004
- Augst, A. D., Barratt, D. C., Hughes, A. D., Glor, F. P., Thom, S. A. G., and Xu, X. Y. (2003). Accuracy and reproducibility of CFD predicted wall shear stress using 3D ultrasound images. *J. Biomech. Eng.* 125, 218–222. doi: 10.1115/1.1553973
- Babuska, I., and Oden, J. (2004). Verification and validation in computational engineering and science: basic concepts. *Comput. Methods Appl. Mech. Eng.* 193, 4057–4066. doi: 10.1016/j.cma.2004.03.002
- Bederson, J. B., Awad, I. A., Wiebers, D. O., Piegras, D., Haley, J., Brott, T., et al. (2000). Recommendations for the management of patients with unruptured intracranial aneurysms: a statement for healthcare professionals from the Stroke Council of the American Heart Association. *Circulation* 102, 2300–2308. doi: 10.1161/01.CIR.102.18.2300
- Berg, P., Roloff, C., Beuing, O., Voss, S., Sugiyama, S.-I., Aristokleous, N., et al. (2015). The computational fluid dynamics rupture challenge 2013–phase II: variability of hemodynamic simulations in two intracranial aneurysms. *J. Biomech. Eng.* 137:121008. doi: 10.1115/1.4031794
- Berg, P., Voß, S., Janiga, G., Saalfeld, S., Bergersen, A. W., Valen-Sendstad, K., et al. (2019). Multiple aneurysms anatomy challenge 2018 (MATCH)-phase II: rupture risk assessment. *Int. J. Comput. Assist. Radiol. Surg.* 14, 1795–1804. doi: 10.1007/s11548-019-01986-2
- Berg, P., Voß, S., Saalfeld, S., Janiga, G., Bergersen, A. W., Valen-Sendstad, K., et al. (2018). Multiple aneurysms anatomy challenge 2018 (MATCH): phase I: segmentation. *Cardiovasc. Eng. Technol.* 9, 565–581. doi: 10.1007/s13239-018-00376-0
- Biasetti, J., Gasser, T. C., Auer, M., Hedin, U., and Labruto, F. (2010). Hemodynamics of the normal aorta compared to fusiform and saccular abdominal aortic aneurysms with emphasis on a potential thrombus formation mechanism. *Annals Biomed. Eng.* 38, 380–390. doi: 10.1007/s10439-009-9843-6
- Biasetti, J., Hussain, F., and Gasser, T. C. (2011). Blood flow and coherent vortices in the normal and aneurysmatic aortas: a fluid dynamical approach to intra-luminal thrombus formation. *J. R. Soc. Interface* 8, 1449–1461. doi: 10.1098/rsif.2011.0041
- Bonert, M., Leask, R. L., Butany, J., Ethier, C. R., Myers, J. G., Johnston, K. W., et al. (2003). The relationship between wall shear stress distributions and intimal thickening in the human abdominal aorta. *Biomed. Eng. Online* 2:18. doi: 10.1186/1475-925X-2-18
- Boussel, L., Rayz, V., Martin, A., Acevedo-Bolton, G., Lawton, M. T., Higashida, R., et al. (2009). Phase-contrast magnetic resonance imaging measurements in intracranial aneurysms *in vivo* of flow patterns, velocity fields, and wall shear stress: comparison with computational fluid dynamics. *Magn. Reson. Med.* 61, 409–417. doi: 10.1002/mrm.21861
- Boussel, L., Rayz, V., McCulloch, C., Martin, A., Acevedo-bolton, G., Lawton, M., et al. (2008). Aneurysm growth occurs at region of low wall shear stress:

- patient-specific correlation of hemodynamics and growth in a longitudinal study. *Stroke* 39, 2997–3002. doi: 10.1161/STROKEAHA.108.521617
- Boyd, A. J. (2020). Biomechanical prediction of abdominal aortic aneurysm rupture potential. *J. Vasc. Surg.* 71, 627. doi: 10.1016/j.jvs.2019.03.052
- Boyd, A. J., Kuhn, D. C., Lozowy, R. J., and Kulbisky, G. P. (2016). Low wall shear stress predominates at sites of abdominal aortic aneurysm rupture. *J. Vasc. Surg.* 63, 1613–1619. doi: 10.1016/j.jvs.2015.01.040
- Campobasso, R., Condemni, F., Viallon, M., Croisille, P., Campisi, S., and Avril, S. (2018). Evaluation of peak wall stress in an ascending thoracic aortic aneurysm using FSI simulations: effects of aortic stiffness and peripheral resistance. *Cardiovasc. Eng. Technol.* 9, 707–722. doi: 10.1007/s13239-018-00385-z
- Canchi, T., Kumar, S. D., Ng, E. Y., and Narayanan, S. (2015). A review of computational methods to predict the risk of rupture of abdominal aortic aneurysms. *Biomed Res. Int.* 2015, 1–12. doi: 10.1155/2015/861627
- Cebral, J. R., Hendrickson, S., and Putman, C. M. (2009). Hemodynamics in a lethal basilar artery aneurysm just before its rupture. *Am. J. Neuroradiol.* 30, 95–98. doi: 10.3174/ajnr.A1312
- Cebral, J. R., Mut, F., Raschi, M., Scrivano, E., Ceratto, R., Lylyk, P., et al. (2011a). Aneurysm rupture following treatment with flow-diverting stents: computational hemodynamics analysis of treatment. *Am. J. Neuroradiol.* 32, 27–33. doi: 10.3174/ajnr.A2398
- Cebral, J. R., Mut, F., Weir, J., and Putman, C. (2011b). Quantitative characterization of the hemodynamic environment in ruptured and unruptured brain aneurysms. *Am. J. Neuroradiol.* 32, 145–151. doi: 10.3174/ajnr.A2419
- Chaikof, E. L., Dalman, R. L., Eskandari, M. K., Jackson, B. M., Lee, W. A., Mansour, M. A., et al. (2018). The Society for Vascular Surgery practice guidelines on the care of patients with an abdominal aortic aneurysm. *J. Vasc. Surg.* 67, 2–77. doi: 10.1016/j.jvs.2017.10.044
- Chalouhi, N., Ali, M. S., Jabbour, P. M., Tjoumakaris, S. I., Gonzalez, L. F., Rosenwasser, R. H., et al. (2012). Biology of intracranial aneurysms: role of inflammation. *J. Cereb. Blood Flow Metab.* 32, 1659–1676. doi: 10.1038/jcbfm.2012.84
- Chung, T. K., da Silva, E. S., and Raghavan, S. M. (2017). Does elevated wall tension cause aortic aneurysm rupture? Investigation using a subject-specific heterogeneous model. *J. Biomech.* 64, 164–171. doi: 10.1016/j.jbiomech.2017.09.041
- Condemni, F., Campisi, S., Viallon, M., Croisille, P., Fuzelier, J. F., and Avril, S. (2018). Ascending thoracic aorta aneurysm repair induces positive hemodynamic outcomes in a patient with unchanged bicuspid aortic valve. *J. Biomech.* 81, 145–148. doi: 10.1016/j.jbiomech.2018.09.022
- Czerny, M., Schmidli, J., Adler, S., Van Den Berg, J. C., Bertoglio, L., Carrel, T., et al. (2019). Current options and recommendations for the treatment of thoracic aortic pathologies involving the aortic arch. *Eur. J. Cardio Thorac. Surg.* 55, 133–162. doi: 10.1093/ejcts/ezy313
- Danad, I., Szymonifka, J., Twis, J. W. R., Norgaard, B. L., Zarins, C. K., Knaapen, P., et al. (2017). Diagnostic performance of cardiac imaging methods to diagnose ischaemia-causing coronary artery disease when directly compared with fractional flow reserve as a reference standard: a meta-analysis. *Eur. Heart J.* 38, 991–998. doi: 10.1093/eurheartj/ehw095
- Dawson, J., and Fitridge, R. (2013). Update on aneurysm disease: current insights and controversies: peripheral aneurysms: when to intervene—is rupture really a danger? *Prog. Cardiovasc. Dis.* 56, 26–35. doi: 10.1016/j.pcad.2013.05.002
- Detmer, F. J., Fajardo-Jiménez, D., Mut, F., Juchler, N., Hirsch, S., Pereira, V. M., et al. (2018a). External validation of cerebral aneurysm rupture probability model with data from two patient cohorts. *Acta Neurochirurg.* 160, 2425–2434. doi: 10.1007/s00701-018-3712-8
- Detmer, F. J., Jae Chung, B., Mut, F., Slawski, M., Hamzei-Sichani, F., Putman, C., et al. (2018b). Development and internal validation of an aneurysm rupture probability model based on patient characteristics and aneurysm location, morphology, and hemodynamics. *Int. J. Comput. Assist. Radiol. Surg.* 13, 1767–1779. doi: 10.1007/s11548-018-1837-0
- Edlin, J., Youssefi, P., Bilkhu, R., Figueroa, C. A., Morgan, R., Nowell, J., et al. (2019). Haemodynamic assessment of bicuspid aortic valve aortopathy: a systematic review of the current literature. *Eur. J. Cardio Thorac. Surg.* 55, 610–617. doi: 10.1093/ejcts/ezy312
- Einstein, A. J., Henzlova, M. J., and Rajagopalan, S. (2007). Estimating risk of cancer associated with radiation exposure from 64-slice computed tomography coronary angiography. *J. Am. Med. Assoc.* 298, 317–323. doi: 10.1001/jama.298.3.317
- Eker, O. F., Boudjeltia, K. Z., Jerez, R. A., Le Bars, E., Sanchez, M., Bonafé, A., et al. (2015). MR derived volumetric flow rate waveforms of internal carotid artery in patients treated for unruptured intracranial aneurysms by flow diversion technique. *J. Cereb. Blood Flow Metab.* 35, 2070–2079. doi: 10.1038/jcbfm.2015.176
- Enevoldsen, M. S., Pedersen, M. M., Hemmsen, M. C., Nielsen, M. B., and Jensen, J. A. (2012). “Computational fluid dynamics using *in vivo* ultrasound blood flow measurements,” in *2012 IEEE International Ultrasonics Symposium, IUS (Dresden)*, 1596–1599. doi: 10.1109/ULTSYM.2012.0399
- Erbel, R., Aboyans, V., Boileau, C., Bossone, E., Di Bartolomeo, R., Eggebrecht, H., et al. (2014). 2014 ESC guidelines on the diagnosis and treatment of aortic diseases. *Eur. Heart J.* 35, 2873–2926. doi: 10.1093/eurheartj/ehu281
- Etminan, N., and Macdonald, R. L. (2015). Computational fluid dynamics and intracranial aneurysms: higher mathematics meets complex biology. *World Neurosurg.* 83, 1017–1019. doi: 10.1016/j.wneu.2015.02.015
- Fan, T., Zhou, Z., Fang, W., Wang, W., Xu, L., and Huo, Y. (2019). Morphometry and hemodynamics of coronary artery aneurysms caused by atherosclerosis. *Atherosclerosis* 284, 187–193. doi: 10.1016/j.atherosclerosis.2019.03.001
- Fiorella, D., Sadasivan, C., Woo, H. H., and Lieber, B. (2011). Regarding “aneurysm rupture following treatment with flow-diverting stents: computational hemodynamics analysis of treatment”. *Am. J. Neuroradiol.* 32:E95. doi: 10.3174/ajnr.A2534
- Grande Gutierrez, N., Kahn, A., Burns, J. C., and Marsden, A. L. (2017). Computational blood flow simulations in Kawasaki disease patients: insight into coronary artery aneurysm hemodynamics. *Glob. Cardiol. Sci. Pract.* 2017:e201729. doi: 10.21542/gcsp.2017.29
- Grande Gutierrez, N., Mathew, M., McCrindle, B. W., Tran, J. S., Kahn, A. M., Burns, J. C., et al. (2019). Hemodynamic variables in aneurysms are associated with thrombotic risk in children with Kawasaki disease. *Int. J. Cardiol.* 281, 15–21. doi: 10.1016/j.ijcard.2019.01.092
- Hendel, A., Ang, L. S., and Granville, D. J. (2015). Inflammation and proteases in abdominal aortic aneurysm. *Curr. Vasc. Pharmacol.* 13, 95–110. doi: 10.2174/157016111301150303132348
- Hiratzka, L. F., Bakris, G. L., Beckman, J. A., Bersin, R. M., Carr, V. F., Casey, D. E., et al. (2009). ACCF/AHA Guideline 2010 ACCF/AHA/AATS/ACR/ASA/SCA/SCAI/SIR/STS/SVM guidelines for the diagnosis and management of patients with thoracic aortic disease ACCF/AHA task force members. *Circulation* 121, 266–369. doi: 10.1161/CIR.0b013e3181d4739e
- Howard, D. P., Banerjee, A., Fairhead, J. F., Handa, A., Silver, L. E., and Rothwell, P. M. (2015). Age-specific incidence, risk factors and outcome of acute abdominal aortic aneurysms in a defined population. *Br. J. Surg.* 102, 907–915. doi: 10.1002/bjs.9838
- Huang, Y. K., Hsieh, H. C., Tsai, F. C., Chang, S. H., Lu, M. S., and Ko, P. J. (2007). Visceral artery aneurysm: risk factor analysis and therapeutic opinion. *Eur. J. Vasc. Endovasc. Surg.* 33, 293–301. doi: 10.1016/j.ejvs.2006.09.016
- Isselbacher, E. M. (2005). Thoracic and abdominal aortic aneurysms. *Circulation* 111, 816–828. doi: 10.1161/01.CIR.0000154569.08857.7A
- Janiga, G., Berg, P., Sugiyama, S., Kono, K., and Steinman, D. A. (2015). The computational fluid dynamics rupture challenge 2013-phase I: prediction of rupture status in intracranial aneurysms. *Am. J. Neuroradiol.* 36:530. doi: 10.3174/ajnr.A4157
- Jia, Y., Morrison, J. C., Tokayer, J., Tan, O., Lombardi, L., Baumann, B., et al. (2012). Quantitative OCT angiography of optic nerve head blood flow. *Biomed. Opt. Express* 3:3127. doi: 10.1364/BOE.3.003127
- Kallmes, D. F. (2012). Point: CFD—computational fluid dynamics or confounding factor dissemination. *AJNR Am. J. Neuroradiol.* 33, 395–396. doi: 10.3174/ajnr.A2993
- Kawaguchi, T., Nishimura, S., Kanamori, M., Takazawa, H., Omodaka, S., Sato, K., et al. (2012). Distinctive flow pattern of wall shear stress and oscillatory shear index: similarity and dissimilarity in ruptured and unruptured cerebral aneurysm blebs. *J. Neurosurg.* 117, 774–780. doi: 10.3171/2012.7.JNS111991
- Kontopodis, N., Pantidis, D., Dedes, A., Daskalakis, N., and Ioannou, C. V. (2016). The-not so-solid 5.5 cm threshold for abdominal aortic aneurysm repair: facts, misinterpretations, and future directions. *Front. Surg.* 3:1. doi: 10.3389/fsurg.2016.00001

- Kumar, V., Abbas, A. K., and Aster, J. C. (2018). *Robbins Basic Pathology*. 10th Edn. Philadelphia, PA: Elsevier.
- Kung, E., Kahn, A. M., Burns, J. C., and Marsden, A. (2014). *In vitro* validation of patient-specific hemodynamic simulations in coronary aneurysms caused by Kawasaki disease. *Cardiovasc. Eng. Technol.* 5, 189–201. doi: 10.1007/s13239-014-0184-8
- Kung, E. O., Les, A. S., Medina, F., Wicker, R. B., McConnell, M. V., and Taylor, C. A. (2011). *In vitro* validation of finite-element model of AAA hemodynamics incorporating realistic outlet boundary conditions. *J. Biomech. Eng.* 133:041003. doi: 10.1115/1.4003526
- Li, D., Ma, J., Wei, C., Zhao, J., Yuan, D., and Zheng, T. (2019). Hemodynamic analysis to assist treatment strategies in complex visceral arterial pathologies: case reports and discussion from pancreaticoduodenal artery aneurysm with superior mesenteric artery occlusion. *Ann. Vasc. Surg.* 59, 1–308. doi: 10.1016/j.avsg.2019.02.049
- Liang, L., Steinman, D. A., Brina, O., Chnafa, C., Cancelliere, N. M., and Pereira, M. (2019). Towards the clinical utility of CFD for assessment of intracranial aneurysm rupture—a systematic review and novel parameter-ranking tool hemorrhagic stroke. *J. Neurointervent Surg.* 11, 153–158. doi: 10.1136/neurintsurg-2018-014246
- Longo, M., Granata, F., Racchiusa, S., Mormina, E., Grasso, G., Longo, G. M., et al. (2017). Role of hemodynamic forces in unruptured intracranial aneurysms: an overview of a complex scenario. *World Neurosurg.* 105, 632–642. doi: 10.1016/j.wneu.2017.06.035
- Machi, P., Ouared, R., Brina, O., Bouillot, P., Yilmaz, H., Vargas, M. I., et al. (2017). Hemodynamics of focal versus global growth of small cerebral aneurysms. *Clin. Neuroradiol.* 29, 285–293. doi: 10.1007/s00062-017-0640-6
- Maher, G., Wilson, N., and Marsden, A. (2019). Accelerating cardiovascular model building with convolutional neural networks. *Med. Biol. Eng. Comput.* 57, 2319–2335. doi: 10.1007/s11517-019-02029-3
- McCord, B. W., Rowley, A. H., Newburger, J. W., Burns, J. C., Bolger, A. F., Gewitz, M., et al. (2017). Diagnosis, treatment, and long-term management of Kawasaki disease: a scientific statement for health professionals from the American Heart Association. *Circulation* 135, e927–e999. doi: 10.1161/CIR.0000000000000484
- McGloughlin, T. M., and Doyle, B. J. (2010). New approaches to abdominal aortic aneurysm rupture risk assessment: engineering insights with clinical gain. *Arterioscler. Thromb. Vasc. Biol.* 30, 1687–1694. doi: 10.1161/ATVBAHA.110.204529
- Mendez, V., Di Giuseppe, M., and Pasta, S. (2018). Comparison of hemodynamic and structural indices of ascending thoracic aortic aneurysm as predicted by 2-way FSI, CFD rigid wall simulation and patient-specific displacement-based FEA. *Comput. Biol. Med.* 100, 221–229. doi: 10.1016/j.compbiomed.2018.07.013
- Meng, H., Tutino, V. M., Xiang, J., and Siddiqui, A. (2014). High WSS or low WSS? Complex interactions of hemodynamics with intracranial aneurysm initiation, growth, and rupture: toward a unifying hypothesis. *Am. J. Neuroradiol.* 35, 1254–1262. doi: 10.3174/ajnr.A3558
- Milewicz, D. M., Guo, D.-C., Tran-Fadulu, V., Lafont, A. L., Papke, C. L., Inamoto, S., et al. (2008). Genetic basis of thoracic aortic aneurysms and dissections: focus on smooth muscle cell contractile dysfunction. *Annu. Rev. Genom. Hum. Genet.* 9, 283–302. doi: 10.1146/annurev.genom.8.080706.092303
- Miura, Y., Ishida, F., Umeda, Y., Tanemura, H., Suzuki, H., Matsushima, S., et al. (2013). Low wall shear stress is independently associated with the rupture status of middle cerebral artery aneurysms. *Stroke* 44, 519–521. doi: 10.1161/STROKEAHA.112.675306
- Numata, S., Itatani, K., Kanda, K., Doi, K., Yamazaki, S., Morimoto, K., et al. (2016). Blood flow analysis of the aortic arch using computational fluid dynamics. *Eur. J. Cardio Thorac. Surg.* 49, 1578–1585. doi: 10.1093/ejcts/ezv459
- Pape, L. A., Tsai, T. T., Isselbacher, E. M., Oh, J. K., O’Gara, P. T., Evangelista, A., et al. (2007). Aortic diameter ≥ 5.5 cm is not a good predictor of type A aortic dissection: observations from the International Registry of Acute Aortic Dissection (IRAD). *Circulation* 116, 1120–1127. doi: 10.1161/CIRCULATIONAHA.107.702720
- Parker, L. P., Powell, J. T., Kelsey, L. J., Lim, B., Ashleigh, R., Venermo, M., et al. (2019). Morphology and hemodynamics in isolated common iliac artery aneurysms impacts proximal aortic remodeling. *Arterioscler. Thromb. Vasc. Biol.* 39, 1125–1136. doi: 10.1161/ATVBAHA.119.312687
- Patel, M. R., Nørgaard, B. L., Fairbairn, T. A., Nieman, K., Akasaka, T., Berman, D. S., et al. (2020). 1-Year impact on medical practice and clinical outcomes of FFRCT: the ADVANCE registry. *JACC Cardiovasc. Imaging* 13, 97–105. doi: 10.1016/j.jcmg.2019.03.003
- Phillips, E. H., Di Achille, P., Bersi, M. R., Humphrey, J. D., and Goergen, C. J. (2017). Multi-modality imaging enables detailed hemodynamic simulations in dissecting aneurysms in mice. *IEEE Trans. Med. Imaging* 36, 1297–1305. doi: 10.1109/TMI.2017.2664799
- Pinard, A., Jones, G. T., and Milewicz, D. M. (2019). Genetics of thoracic and abdominal aortic diseases. *Circ. Res.* 124, 588–606. doi: 10.1161/CIRCRESAHA.118.312436
- Putman, C. M., Lylyk, P., and Czeisler, J. (2011). Reply. *Am. J. Neuroradiol.* 32, E98–E100. doi: 10.3174/ajnr.A2560
- Qiu, T., Jin, G., Xing, H., and Lu, H. (2017). Association between hemodynamics, morphology, and rupture risk of intracranial aneurysms: a computational fluid modeling study. *Neurol. Sci.* 38, 1009–1018. doi: 10.1007/s10072-017-2904-y
- Qiu, Y., Yuan, D., Wang, Y., Wen, J., and Zheng, T. (2018). Hemodynamic investigation of a patient-specific abdominal aortic aneurysm with iliac artery tortuosity. *Comput. Methods Biomech. Biomed. Eng.* 21, 824–833. doi: 10.1080/10255842.2018.1522531
- Ramanath, V. S., Oh, J. K., Sundt, T. M., and Eagle, K. A. (2009). Acute aortic syndromes and thoracic aortic aneurysm. *Mayo Clin. Proc.* 84, 465–481. doi: 10.1016/S0025-6196(11)60566-1
- Rayz, V. L., Bousset, L., Ge, L., Leach, J. R., Martin, A. J., Lawton, M. T., et al. (2010). Flow residence time and regions of intraluminal thrombus deposition in intracranial aneurysms. *Ann. Biomed. Eng.* 38, 3058–3069. doi: 10.1007/s10439-010-0065-8
- Reymond, P., Crosetto, P., Deparis, S., Quarteroni, A., and Stergiopoulos, N. (2013). Physiological simulation of blood flow in the aorta: comparison of hemodynamic indices as predicted by 3-D FSI, 3-D rigid wall and 1-D models. *Med. Eng. Phys.* 35, 784–791. doi: 10.1016/j.medengphy.2012.08.009
- Reza, M. M. S., and Arzani, A. (2019). A critical comparison of different residence time measures in aneurysms. *J. Biomech.* 88, 122–129. doi: 10.1016/j.jbiomech.2019.03.028
- Roache, P. J. (1994). Perspective: a method for uniform reporting of grid refinement studies. *J. Fluids Eng.* 116, 405–413. doi: 10.1115/1.2910291
- Roache, P. J. (1997). Quantification of uncertainty in computational fluid dynamics. *Annu. Rev. Fluid Mech.* 29, 123–160. doi: 10.1146/annurev.fluid.29.1.123
- Saeyeldin, A., Zafar, M. A., Li, Y., Tanweer, M., Abdelbaky, M., Gryaznov, A., et al. (2019). Decision-making algorithm for ascending aortic aneurysm: effectiveness in clinical application? *J. Thorac. Cardiovasc. Surg.* 157, 1733–1745. doi: 10.1016/j.jtcvs.2018.09.124
- Sailer, A. M. H., Wagemans, B. A. J. M., Nelemans, P. J., De Graaf, R., and Van Zwam, W. H. (2014). Diagnosing intracranial aneurysms with mr angiography: systematic review and meta-analysis. *Stroke* 45, 119–126. doi: 10.1161/STROKEAHA.113.003133
- Salman, H. E., Ramazanli, B., Yavuz, M. M., and Yalcin, H. C. (2019). Biomechanical investigation of disturbed hemodynamics-induced tissue degeneration in abdominal aortic aneurysms using computational and experimental techniques. *Front. Bioeng. Biotechnol.* 7:111. doi: 10.3389/fbioe.2019.00111
- Saqr, K. M., Rashad, S., Tupin, S., Niizuma, K., Hassan, T., Tominaga, T., et al. (2019). What does computational fluid dynamics tell us about intracranial aneurysms? A meta-analysis and critical review. *J. Cereb. Blood Flow Metab.* 40, 1021–1039. doi: 10.1177/0271678X19854640
- Sei, Y. J., Ahn, S. I., Virtue, T., Kim, T., and Kim, Y. (2017). Detection of frequency-dependent endothelial response to oscillatory shear stress using a microfluidic transcellular monitor. *Sci. Rep.* 7:10019. doi: 10.1038/s41598-017-10636-z
- Sengupta, D. (2013). *Risk assessment using image-based hemodynamic modeling of patients with coronary artery aneurysms caused by Kawasaki disease* (Ph.D. thesis), University of California, San Diego, San Diego, CA, United States.
- Sengupta, D., Kahn, A. M., Burns, J. C., Sankaran, S., Shadden, S. C., and Marsden, A. L. (2012). Image-based modeling of hemodynamics in coronary artery aneurysms caused by Kawasaki disease. *Biomech. Model. Mechanobiol.* 11, 915–932. doi: 10.1007/s10237-011-0361-8
- Sengupta, D., Kahn, A. M., Kung, E., Esmaily Moghadam, M., Shirinsky, O., Lyskina, G. A., et al. (2014). Thrombotic risk stratification using

- computational modeling in patients with coronary artery aneurysms following Kawasaki disease. *Biomech. Model. Mechanobiol.* 13, 1261–1276. doi: 10.1007/s10237-014-0570-z
- Shi, Y., Zhu, M., Chang, Y., Qiao, H., and Liu, Y. (2016). The risk of stanford type-A aortic dissection with different tear size and location: a numerical study. *Biomed. Eng. Online* 15:128. doi: 10.1186/s12938-016-0258-y
- Shojima, M., Nemoto, S., Morita, A., Oshima, M., Watanabe, E., and Saito, N. (2010). Role of shear stress in the blister formation of cerebral aneurysms. *Neurosurgery* 67, 1268–1274. doi: 10.1227/NEU.0b013e3181f2f442
- Singh, P. K., Marzo, A., Coley, S. C., Berti, G., Bijlenga, P., Lawford, P. V., et al. (2009). The role of computational fluid dynamics in the management of unruptured intracranial aneurysms: a clinicians' view. *Comput. Intell. Neurosci.* 2009:760364. doi: 10.1155/2009/760364
- Soudah, E., Ng, E. Y., Loong, T. H., Bordone, M., Pua, U., and Narayanan, S. (2013). CFD modelling of abdominal aortic aneurysm on hemodynamic loads using a realistic geometry with CT. *Comput. Math. Methods Med.* 2013, 1–9. doi: 10.1155/2013/472564
- Steinman, D. A. (2011). Computational modeling and flow diverters: a teaching moment. *Am. J. Neuroradiol.* 32, 981–983. doi: 10.3174/ajnr.A2711
- Steinman, D. A., Hoi, Y., Fahy, P., Morris, L., Walsh, M. T., Aristokleous, N., et al. (2013). Variability of computational fluid dynamics solutions for pressure and flow in a giant aneurysm: the ASME 2012 summer bioengineering conference CFD challenge. *J. Biomech. Eng.* 135:021016. doi: 10.1115/1.4023382
- Steinman, D. A., and Migliavacca, F. (2018). Editorial: Special issue on verification, validation, and uncertainty quantification of cardiovascular models: towards effective VUQ for translating cardiovascular modelling to clinical utility. *Cardiovasc. Eng. Technol.* 9, 539–543. doi: 10.1007/s13239-018-00393-z
- Steinman, D. A., and Pereira, V. M. (2019). How patient specific are patient-specific computational models of cerebral aneurysms? An overview of sources of error and variability. *Neurosurg. Focus* 47:E14. doi: 10.3171/2019.4.FOCUS19123
- Sugiyama, S., Niizuma, K., Nakayama, T., Shimizu, H., Endo, H., Inoue, T., et al. (2013). Relative residence time prolongation in intracranial aneurysms: a possible association with atherosclerosis. *Neurosurgery* 73, 767–776. doi: 10.1227/NEU.0000000000000096
- Suh, S.-H., Kim, H.-H., Choi, Y. H., and Lee, J. S. (2012). Computational fluid dynamic modeling of femoral artery pseudoaneurysm. *J. Mech. Sci. Technol.* 26, 3865–3872. doi: 10.1007/s12206-012-1012-4
- Taylor, C., Kim, H. J., Choi, G., Roy, A., Khem, S., Schaap, M., et al. (2018). “Modeling blood flow and pressure in the coronary arteries: from the academy to the clinic”, in *8th World Congress of Biomechanics* (Dublin).
- Taylor, C. A., and Steinman, D. A. (2010). Image-based modeling of blood flow and vessel wall dynamics: applications, methods and future directions: sixth international bio-fluid mechanics symposium and workshop, March 28–30, 2008 Pasadena, California. *Ann. Biomed. Eng.* 38, 1188–1203. doi: 10.1007/s10439-010-9901-0
- Thompson, B. G., Brown, R. D., Amin-Hanjani, S., Broderick, J. P., Cockroft, K. M., Connolly, E. S., et al. (2015). Guidelines for the management of patients with unruptured intracranial aneurysms: a guideline for healthcare professionals from the American Heart Association/American Stroke Association. *Stroke* 46, 2368–2400. doi: 10.1161/STR.0000000000000070
- Tian, Z., Zhang, Y., Jing, L., Liu, J., Zhang, Y., and Yang, X. (2016). Rupture risk assessment for mirror aneurysms with different outcomes in the same patient. *Front. Neurol.* 7:219. doi: 10.3389/fneur.2016.00219
- Torii, R., Oshima, M., Kobayashi, T., Takagi, K., and Tezduyar, T. E. (2007). Influence of wall elasticity in patient-specific hemodynamic simulations. *Comput. Fluids* 36, 160–168. doi: 10.1016/j.compfluid.2005.07.014
- Trachet, B., Bols, J., Degroote, J., Verheghe, B., Stergiopoulos, N., Vierendeels, J., et al. (2015). An animal-specific FSI model of the abdominal aorta in anesthetized mice. *Ann. Biomed. Eng.* 43, 1298–1309. doi: 10.1007/s10439-015-1310-y
- UCAS Japan Investigators, Morita, A., Kirino, T., Hashi, K., Aoki, N., Fukuhara, S., Hashimoto, N., et al. (2012). The natural course of unruptured cerebral aneurysms in a Japanese cohort. *N. Engl. J. Med.* 366, 2474–2482. doi: 10.1056/NEJMoa1113260
- Valen-Sendstad, K., Bergersen, A. W., Shimogonya, Y., Goubergrits, L., Bruening, J., Pallares, J., et al. (2018). Real-world variability in the prediction of intracranial aneurysm wall shear stress: the 2015 international aneurysm CFD challenge. *Cardiovasc. Eng. Technol.* 9, 544–564. doi: 10.1007/s13239-018-00374-2
- Vali, A., Abla, A. A., Lawton, M. T., Saloner, D., and Rayz, V. L. (2017). Computational fluid dynamics modeling of contrast transport in basilar aneurysms following flow-altering surgeries. *J. Biomech.* 50, 195–201. doi: 10.1016/j.jbiomech.2016.11.028
- Van Disseldorp, E. M., Petterson, N. J., Van De Vosse, F. N., Van Sambeek, M. R., and Lopata, R. G. (2019). Quantification of aortic stiffness and wall stress in healthy volunteers and abdominal aortic aneurysm patients using time-resolved 3D ultrasound: a comparison study. *Eur. Heart J. Cardiovasc. Imaging* 20, 185–191. doi: 10.1093/ehjci/jev051
- VASCOPS (2018). *VASCOPS-Products/Service*.
- Vorp, D. A. (2007). Biomechanics of abdominal aortic aneurysm. *J. Biomech.* 40, 1887–1902. doi: 10.1016/j.jbiomech.2006.09.003
- Voß, S., Beuing, O., Janiga, G., and Berg, P. (2019). Multiple aneurysms anatomy challenge 2018 (MATCH)-phase Ib: effect of morphology on hemodynamics. *PLoS ONE* 14:e0216813. doi: 10.1371/journal.pone.0216813
- Wan, H., Ge, L., Huang, L., Jiang, Y., Leng, X., Feng, X., et al. (2019). Sidewall aneurysm geometry as a predictor of rupture risk due to associated abnormal hemodynamics. *Front. Neurol.* 10:841. doi: 10.3389/fneur.2019.00841
- Wanhainen, A., Verzini, F., Van Herzele, I., Allaire, E., Bown, M., Cohnert, T., et al. (2019). Editor's Choice–European Society for Vascular Surgery (ESVS) 2019 clinical practice guidelines on the management of abdominal aorto-iliac artery aneurysms. *Eur. J. Vasc. Endovasc. Surg.* 57, 8–93. doi: 10.1016/j.ejvs.2018.09.020
- Xiang, J., Natarajan, S. K., Tremmel, M., Ma, D., Mocco, J., Hopkins, L. N., et al. (2011). Hemodynamic-morphologic discriminants for intracranial aneurysm rupture. *Stroke* 42, 144–152. doi: 10.1161/STROKEAHA.110.592923
- Yamaguchi, R. (2016). Effect of elasticity on flow characteristics inside intracranial aneurysms. *Int. J. Neurol. Neurother.* 3:049. doi: 10.23937/2378-3001/3/3/1049
- Youssefi, P., Sharma, R., Figueroa, C. A., and Jahangiri, M. (2017). Functional assessment of thoracic aortic aneurysms—the future of risk prediction? *Br. Med. Bull.* 121, 61–71. doi: 10.1093/bmb/dw049
- Zafar, M. A., Li, Y., Rizzo, J. A., Charilaou, P., Saeyeldin, A., Velasquez, C. A., et al. (2018). Height alone, rather than body surface area, suffices for risk estimation in ascending aortic aneurysm. *J. Thorac. Cardiovasc. Surg.* 155, 1938–1950. doi: 10.1016/j.jtcvs.2017.10.140
- Zhang, Y., Tian, Z., Jing, L., Zhang, Y., Liu, J., and Yang, X. (2016). Bifurcation type and larger low shear area are associated with rupture status of very small intracranial aneurysms. *Front. Neurol.* 7:169. doi: 10.3389/fneur.2016.00169

Conflict of Interest: The authors declare that the research was conducted in the absence of any commercial or financial relationships that could be construed as a potential conflict of interest.

Copyright © 2020 Lipp, Niedert, Cebull, Diorio, Ma, Rothenberger, Stevens Boster and Goergen. This is an open-access article distributed under the terms of the Creative Commons Attribution License (CC BY). The use, distribution or reproduction in other forums is permitted, provided the original author(s) and the copyright owner(s) are credited and that the original publication in this journal is cited, in accordance with accepted academic practice. No use, distribution or reproduction is permitted which does not comply with these terms.